

# Multi Carrier Based PWM for Quasi-Z-Source Cascade Multilevel Inverter-Based Grid-Tie Single-Phase Photovoltaic Power System

Pulloju Divya Jyothi<sup>1</sup>, Dr. S. Siva Prasad<sup>2</sup>, Mr. R. Suresh Babu<sup>3</sup>

<sup>1</sup>PG Scholar, EEE Dept., JB Institute of Engineering and Technology (UGC Autonomous), Hyderabad.

Email: [divyajyothi46@gmail.com](mailto:divyajyothi46@gmail.com)

<sup>2</sup>Professor & HOD, EEE Dept., JB Institute of Engineering and Technology (UGC Autonomous), Hyderabad

Email: [sshivprasadeee@gmail.com](mailto:sshivprasadeee@gmail.com)

<sup>3</sup>Assoc. Professor, EEE Dept., JB Institute of Engineering and Technology (UGC Autonomous), Hyderabad.

Email: [sbrega123@gmail.com](mailto:sbrega123@gmail.com)

**Abstract--**This paper presents an effective control method, including system-level control and Multi Carrier based pulse width modulation for quasi-Z-source cascade multilevel inverter (qZS-CMI) based grid-tie photovoltaic (PV) power system. A new method of multi-carrier PWM strategies is also proposed and compared with different conventional multi-carrier PWM techniques. Reduction of total harmonics distortion (THD) and improvement of the harmonic spectrum of inverter output voltage are some advantages of the proposed control method. The simulation results based on the MATLAB/SIMULINK software are presented to validate the capabilities of the proposed modulation method.

**Keywords:** Cascade multilevel inverter (CMI), photovoltaic (PV) power system, quasi-Z-source inverter, space vector modulation (SVM). Multilevel inverter; multi-carrier PWM techniques; PD PWM; POD PWM; APODPWM.

## 1. Introduction

A recent upsurge in the study of photovoltaic (PV) power generation emerges, since they directly convert the solar radiation into electric power without hampering the environment. However, the stochastic fluctuation of solar power is inconsistent with the desired stable power injected to the grid, owing to variations of solar irradiation and temperature. To fully exploit the solar energy, extracting the PV panels' maximum power and feeding them into grids at unity power factor become the most important. They possess the advantages of both traditional CMI and Z-source topologies. For example, the ZS/qZS-CMI: 1)has high-quality staircase output voltage waveforms with lower harmonic distortions, and reduces/eliminates output filter requirements for the compliance of grid harmonic standards;2) requires power semiconductors with a lower rating, and greatly saves the costs; 3) shows modular topology that each inverter has the same circuit topology, structure and modulation [1], [2]; 4) most important of all, has independent dc-link voltage compensation with the special voltage step-up/down function in a single-stage power conversion of Z-source/quasi-Z-source network, which allows an independent control of the power delivery with high reliability and5) can fulfill the distributed MPPT [6], [8].In order to properly operate the ZS/qZS-CMI, the power injection, independent control of dc-link voltages, and the pulse width modulation (PWM) are

necessary. The PS-SPWM consumes more resources to achieve the shoot-through states because two more references are compared with the carrier waveform. Additionally, the ZS/qZS-CMI based grid-tie PV system has never been modeled in detail to design the controllers. The main contributions of this paper include: 1) a novel multilevel space vector modulation (SVM) technique for the single phase qZS-CMI is proposed, which is implemented without additional resources; 2) a grid-connected control for the qZS-CMI based PV system is proposed, where the all PV panel voltage references from their independent MPPTs are used to control the grid-tie current; the dual-loop dc-link peak voltage control is employed in every qZS-HBI module to balance the dc-link voltages; 3) the design process of regulators is completely presented to achieve fast response and good stability; and 4) simulation and experimental results verify the proposed PWM algorithm and control scheme. The H-bridge topology was followed by the diode-clamped converter which utilized a bank of series capacitors [6]. Another fundamental multilevel topology, the flying capacitor, involves series connection of clamped switching cells [7]. This topology has several unique and attractive features when compared to the diode-clamped inverter. One feature is that added clamping diodes are not needed. Furthermore, the flying capacitor inverter has switching redundancy within the phase which can be used to balance the flying capacitors so that only one dc source is needed [2]. Different modulation strategies have been used in multilevel power applications within the technical literature. They can generally be classified into three categories: fundamental frequency switching, space vector PWM (SVPWM) and multi-carrier PWM techniques. This paper focused on the multi-carrier PWM technique which has been extended using multiple references Multi-carrier PWM techniques can be categorized into three groups: phase disposition PWM (PD-PWM), phase opposition disposition PWM (POD-PWM) and alternate phase opposition disposition PWM (APOD-PWM) techniques. In these modulation strategies, the reference waveform is sampled through a number of carrier waveforms displayed by contiguous of the reference waveform amplitude [8-11].The different multi-carrier PWM modulation strategies for multilevel inverters will be reviewed in this paper.

## 2. DESCRIPTION OF QZS-CMI-BASED GRID-TIE PV POWER SYSTEM

Fig. 1 shows the discussed qZS-CMI-based grid-tie PV power system. The total output voltage of the inverter is

a series summation of qZS-HBI cell voltages. Each cell is fed by an independent PV panel. The individual PV power source is an array composed of identical PV panels in parallel and series. A typical PV model in [12] is performed by considering both the solar irradiation and the PV panel temperature.

**2.1 qZS-CMI**

The qZS-CMI combines the qZS network into each HBI module. When the Kth qZS-HBI is in non shoot-through states, it will work as a traditional HBI. There are

$$\hat{v}_{DCk} = \frac{1}{1 - 2D_k} v_{PVk} = B_k v_{PVk} \quad v_{Hk} = S_k \hat{v}_{DCk} \quad (1)$$

While in shoot-through states, the qZS-HBI module does not contribute voltage. There are

$$\hat{v}_{DCk} = 0 \quad v_{Hk} = 0. \quad (2)$$

For the qZS-CMI, the synthesized voltage is

$$v_H = \sum_{k=1}^n v_{Hk} = \sum_{k=1}^n S_k \hat{v}_{DCk} \quad (3)$$

Where  $v_{PVk}$  is the output voltage of the th PV array;  $v_{DCk}$  is the dc-link voltage of the th qZS-HBI module;  $D_k$  and  $B_k$  represent the shoot-through duty ratio and boost factor of the Kth qZS-HBI, respectively,  $v_{Hk}$  is the output voltage of the Kth module, and  $S_k$  belongs to  $\{-1,0,1\}$  is the switching function of the Kth qZS-HBI.

**2.2 Control Strategy**

The control objectives of the qZS-CMI based grid-tie PV system are: 1) the distributed MPPT to ensure the maximum power extraction from each PV array; 2) the power injection to the grid at unity power factor with low harmonic distortion; 3) The same dc-link peak voltage for all qZS-HBI modules. The overall control scheme of Fig. 1 is proposed to fulfil these purposes. For achieving the first two goals, the n+ 1 closed loop is employed, as Fig. 1(a) shows.

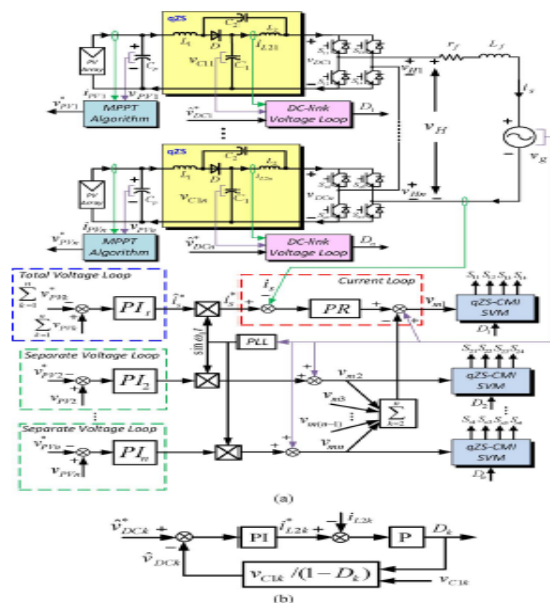


**Fig. 1 (a) qZS-CMI based grid-tie PV power system. (b) DC-link peak voltage control**

1) Total PV array voltage loop adjusts the sum of PV array voltages tracking the sum of PV array voltage references by using a proportional and integral (PI) regulator PI<sub>t</sub>. Each PV array voltage reference is from its MPPT control independently.

2) Grid-tie current loop ensures a sinusoidal grid-injected current in phase with the grid voltage. The total PV array voltage loop outputs the desired amplitude of grid-injected current. A Proportional + Resonant (PR) regulator enforces the actual grid current to track the desired grid-injected reference. The current loop output's total modulation signal subtracts the modulation signal sum of the second, third... and nth qZS-HBI modules to get the first qZS-HBI module's modulation signal.

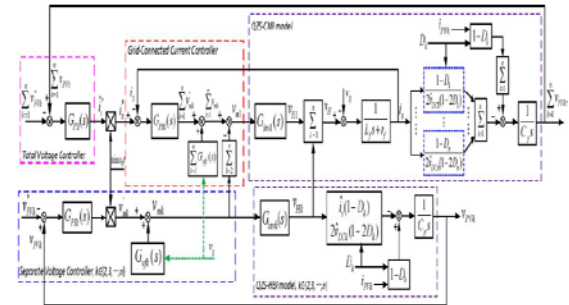


**Fig. 2 Block diagram of the proposed grid-tie control with the model for the qZS-CMI based PV system**

3) The n-1 separate PV array voltage loops regulate the other n-1 PV array voltages to achieve their own MPPTs through the n-1 PI regulators, such as PI<sub>2</sub> to PI<sub>n</sub>, respectively. With the total PV array voltage loop control, the PV arrays fulfil the distributed MPPT. In addition, the voltage feed forward control is used to generate each qZS-HBI module's modulation signal, which will reduce the n regulators' burden, achieve the fast dynamic response, and minimize the grid voltage's impact on the grid-tie current. For the third goal, the dc-link peak voltage is adjusted in terms of its shoot-through duty ratio for each qZS-HBI module, as Fig. 1(b) shows. A proportional ( ) regulator is employed in the inductor L2 current loop to improve the dynamic response, and a PI regulator of the dc-link voltage loop ensures the dc-link peak voltage tracking the reference. Finally, the independent modulation signals  $v_{mk}$  and shoot through duty ratios  $D_k$  of the qZS-CMI,  $k$  belongs to  $\{1,2,\dots,n\}$ , are combined into the proposed multilevel SVM to achieve the desired purposes.

**3. SYSTEM MODELING AND CONTROL**

Fig. 2 shows block diagram of the proposed grid-tie control with the system model for the qZS-CMI based PV power system. The details will be explained as follows.

- Grid-Tie Current Loop

After that the current loop of Fig. 2 is simplified to Fig. 3

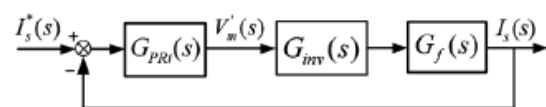


**Fig. 3 Simplified block diagram of the grid-current closed loop**

- PV Voltage Loop

The block diagrams of total and separate PV voltage loops can be obtained in Figs. 4 and 5.

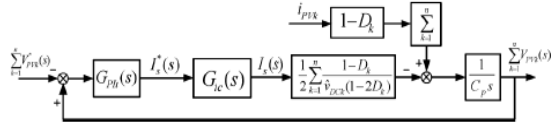


Fig. 4 Block diagram of total PV voltage loop

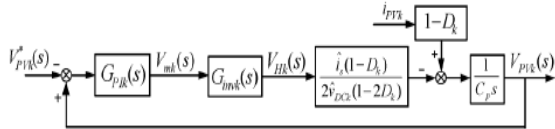


Fig. 5 Block diagram of separate PV voltage loop

- DC-Link Voltage Control

The independent dc-link peak voltage control based on the inductor-L2 current and the capacitor-C1 voltage is performed for each qZS-HBI module, as Fig. 1(b) shows. With the employed proportional regulator at the coefficient for the inductor current loop, as the block diagram of KdPk Fig. 6

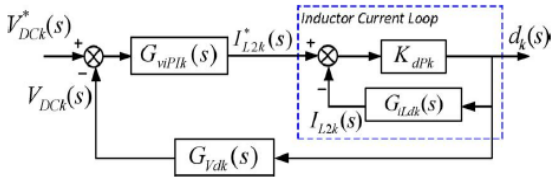


Fig. 6 Block diagram of the Kth module's dc-link peak voltage control

A PI regulator with the transfer function of  $G_{viPIk}(s) = K_{VdPk} + (K_{VdIk}/s)$  is cascaded to the inductor current loop for controlling the dc-link peak voltage, as shown in Fig. 6.

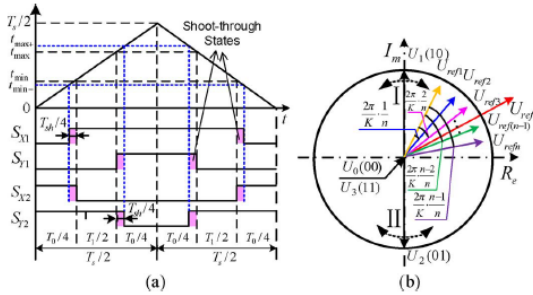


Fig. 7 Proposed multilevel SVM for the single-phase qZS-CMI. (a) Switching pattern of one qZS-HBI module. (b) Synthetization of voltage vectors for the qZS-CMI

#### 4. MULTILEVEL SVM FOR QZS-CMI

Here a delay of the switching times for upper switches or a lead of the switching times for lower switches are employed at the transition moments, as Fig. 7(a) shows. To generate the step-like ac output voltage waveform from the qZS-CMI, a  $2\pi/(nK)$  phase difference, in which K is the number of reference voltage vectors in each

cycle, is employed between any two adjacent voltage vectors, as Fig. 7(b) shows.

#### 4.1 CONTROL PARAMETER DESIGN

The prototype specifications of qZS-CMI based PV power system are shown in Table I. The design results are shown in Table II, and all of the Bode plots are shown in Figs. 8–10. Fig. 8 shows the Bode plots of the grid-tie current loop transfer functions  $G_{io}(s)$  and  $G_{icm}(s)$ , which are before and after compensation, respectively.

TABLE I  
PROTOTYPE SPECIFICATIONS

| Parameters                             | Value        |
|--|--------------|
| Minimum PV array voltage, $V_{PV,min}$ | 60 V         |
| Maximum PV array voltage, $V_{PV,max}$ | 120 V        |
| qZS inductance, $L_1$ and $L_2$        | 1.8 mH       |
| qZS capacitance, $C_1$ and $C_2$       | 3300 $\mu$ F |
| PV array parallel capacitance, $C_p$   | 1100 $\mu$ F |
| Filter inductance, $L_f$               | 1 mH         |
| Carrier frequency, $f_c$               | 5 kHz        |

TABLE II  
CONTROL PARAMETERS

| Parameters | Value     | Parameters | Value   |
|------------|-----------|------------|---------|
| $k_{iP}$   | $5.15e-3$ | $k_{iR}$   | 0.1592  |
| $k_{PV}$   | 1.1464    | $k_{fI}$   | 10.854  |
| $k_{PK}$   | 0.015     | $k_{fK}$   | 0.05256 |
| $k_{dPk}$  | 0.0068    |            |         |
| $k_{VdPk}$ | 0.0281    | $k_{VdK}$  | 2.5254  |

Fig. 9(a) shows the Bode plots of total PV voltage control loop transfer functions  $G_{vot}(s)$  and  $-G_{vcomt}(s)$ , which correspond to before and after compensation, respectively. Similarly, the Bode plots of separate PV voltage control are shown in Fig. 9(b). From Fig. 9(b) and (25), we know that the  $G_{vok}(s)$  is not stable. Compensated by the PI regulator GPIk(s), an 87.5 phase margin is shown in  $-G_{vcomk}(s)$ . The closed-loop transfer function  $G_{vck}(s)$  also confirms its stable feature. Fig. 10 shows the Bode plots of transfer functions for each module's dc-link peak voltage control loop. When using a proportional gain KdPk, the inductor L2 current shows a faster response without loss of the stability, as shown in Fig. 10(a). From Fig. 10(b), the dc-link peak voltage closed-loop's stability is greatly improved by decreasing the crossover frequency. As a result, the closed-loop transfer function  $G_{Vdck}(s)$  presents a fast and robust characteristic.

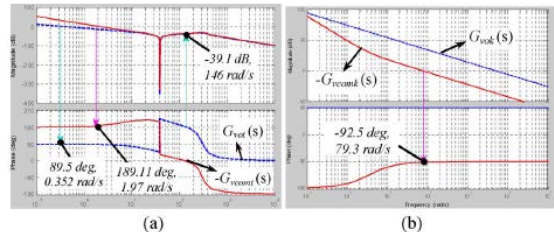


Fig. 9. Bode diagrams of (a)  $G_{vot}(s)$  and  $-G_{vcomt}(s)$ ; and (b)  $G_{vok}(s)$  and  $-G_{vcomk}(s)$ .

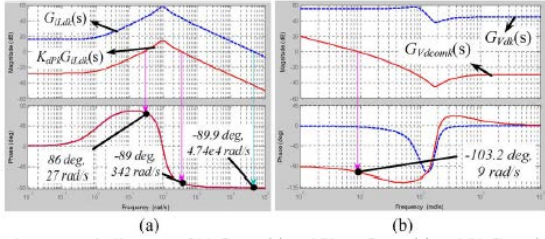


Fig. 10. Bode diagrams of (a)  $G_{iLdk}(s)$  and  $K_{dPk}G_{iLdk}(s)$  and (b)  $G_{Vdk}(s)$  and  $G_{Vdcomk}(s)$ .

#### 4.2 CONVENTIONAL CARRIER-BASED PWM METHODS

Multicarrier PWM techniques entail the natural sampling of a single modulating or reference waveform typically being sinusoidal, through several carrier signals typically being triangular waveforms [9]. In order to describe the different multi-carrier PWM methods the following definitions should be considered:

- The frequency modulation index is defined as  $mf = fc / fr$ , where  $fc$  is the frequency of carrier signals and  $fr$  is the frequency of the reference signal.
- The amplitude modulation index is defined as  $ma = Ar / Ac$ , where  $Ar$  is the amplitude of reference signals and  $Ac$  is the peak to peak value of the carrier signal [8].

The methods are

- PD-PWM method
- POD-PWM method
- APOD-PWM method

#### 4.3 PROPOSED MODULATION METHOD

For reducing the number of carrier signals and also improvement of the THD and harmonic spectrum of inverter output voltage, a new modulation strategy is proposed in this paper. The proposed multi-carrier PWM method uses  $(N - 1) / 2$  carrier signals to generate the  $N$ -level at output voltage. The carrier signals have the same amplitude,  $Ac$  and the same frequency,  $fc$ , and are in phase. The sinusoidal reference wave has a frequency  $fr$  and an amplitude  $Ar$ . In the proposed method, the sinusoidal reference and its inverse are used for generating the required gate signals. The frequency of the output voltage is determined by the frequency of the sinusoidal reference waveform. The amplitude of the fundamental component of the output voltage is determined by the amplitude modulation index,  $ma$ . Fig. 1 shows the proposed multicarrier PWM method for a single-phase 5-level inverter. As this figure shows, the proposed method uses two reference signals and two carrier signals. This method is based on a comparison of the sinusoidal reference waveforms with carrier waveforms. For even and odd values of frequency modulation index,  $mf$ , the significant harmonics are located in two sidebands around the frequency,  $2fc$ . As a result, the frequency spectrum of the output voltage is improved. So, the size of the required filter will be small. It is important to note that the design of filter is not the objective of this work. Reduction of the THD of the output voltage is other important advantage of the proposed method. It is noticeable that the conventional modulation methods generate the significant harmonics in two sidebands around the carrier frequency,  $fc$ .

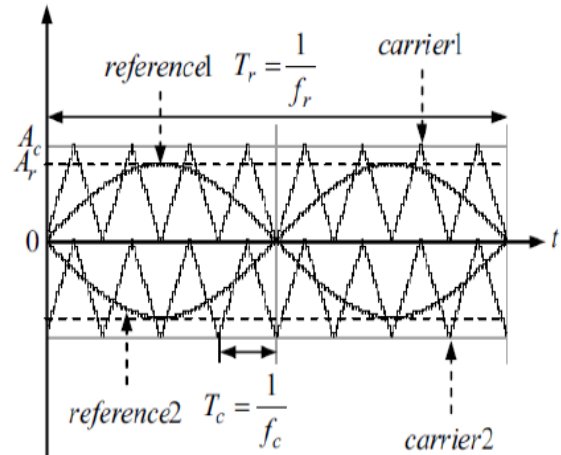


Fig. 11 Proposed multi-carrier PWM method for a single-phase 7-level inverter

#### 5. SIMULATION RESULTS

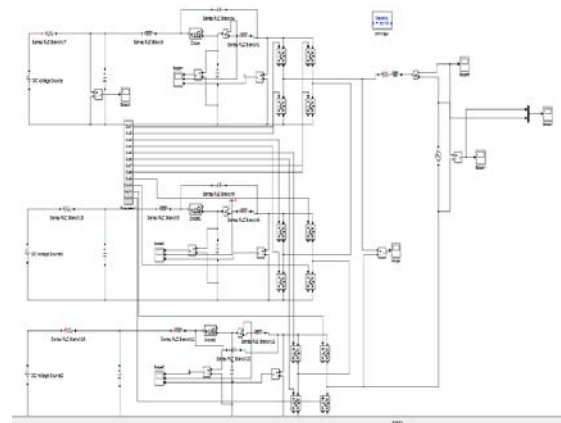


Fig. 12 Simulation of the qZS-CMI

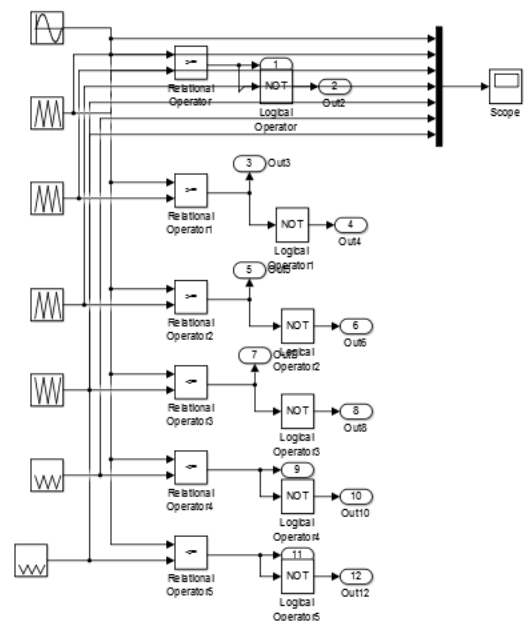
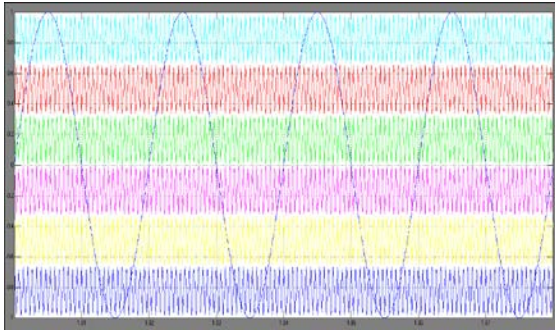
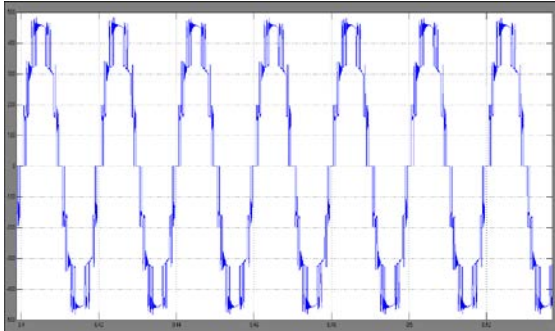


Fig. 13 Simulation of the proposed multi-carrier PWM



**Fig. 14 Proposed multi carriers**



**Fig. 15 7-level output voltage of the qZI**

## 6. CONCLUSION

In this paper, a new method of multi-carrier PWM method is proposed. This paper proposed a control method for qZS-CMI based single-phase grid-tie PV system. The grid-injected power was fulfilled at unity power factor, all qZS-HBI modules separately achieved their own maximum power points tracking even if some modules' PV panels had different conditions. The significant harmonics in conventional methods are located in two sidebands around  $m\omega$  and its multiple. But in the proposed method, the significant harmonics are located in two sidebands around  $2m\omega$  and its multiple. As a result, the size of the required filter will be small. Reduction of the THD of the output voltage is other important advantage of the proposed method in comparison with other conventional multi-carrier PWM methods.

## REFERENCES

[1] SurinKhomfoi and Leon M. Tolbert, "Multilevel Power Converters," *Book Chapter*.  
 [2] R. H. Baker and L. H. Bannister, "Electric power converter," U.S. Patent 3 867 643, Feb. 1975.  
 [3] A. Nabae, I. Takahashi, and H. Akagi, "A new neutral-point clamped PWM inverter," *IEEE Trans. Ind. Appl.*, Vol. IA-17, pp. 518-523, Sep./Oct. 1981.  
 [4] J. Chavarria, D. Biel, F. Guinjoan, C. Meza, and J. J. Negroni, "Energy balance control of PV cascaded multilevel grid-connected inverters under level-shifted and phase-shifted PWMs," *IEEE Trans. Ind. Electron.*, vol. 60, no. 1, pp. 98–111, Jan. 2013.  
 [5] F. Filho, H. Z. Maia, T. H. A. Mateus, B. Ozpineci, L. M. Tolbert, and J. O. P. Pinto, "Adaptive selective harmonic minimization based on ANNs for cascade multilevel inverters with varying DC sources," *IEEE Trans. Ind. Electron.*, vol. 60, no. 5, pp. 1955–1962, May 2013.

[6] S. Kouro, C. Fuentes, M. Perez, and J. Rodriguez, "Single DC-link cascaded H-bridge multilevel multistring photovoltaic energy conversion system with inherent balanced operation," in *Proc. IECON 38th Annu. Conf. IEEE Ind. Electron. Soc.*, Oct. 25–28, 2012, pp. 4998–5005.  
 [7] S. Rivera, S. Kouro, B. Wu, J. I. Leon, J. Rodriguez, and L. G. Franquelo, "Cascaded H-bridge multilevel converter multistring topology for large scale photovoltaic systems," in *Proc. IEEE Int. Symp. Ind. Electron.*, Jun. 27–30, 2011, pp. 1837–1844.  
 [8] L. Liu, H. Li, Y. Zhao, X. He, and Z. J. Shen, "1 MHz cascaded Z-source inverters for scalable grid-interactive photovoltaic (PV) applications using GaN device," in *Proc. IEEE Energy Conv. Congr. Expo.*, Sep. 17–22, 2011, pp. 2738–2745.  
 [9] B. Ge, "Energy Stored Cascade Multilevel Photovoltaic Grid-Tie Power Generation System," China Patent ZL201010234877.0, Jul. 2010, in Chinese.  
 [10] Y. Zhou, L. Liu, and H. Li, "A high-performance photovoltaic module integrated converter (MIC) based on cascaded quasi-Z-source inverters (qZSI) using eGaN FETs," *IEEE Trans. Power Electron.*, vol. 28, no. 6, pp. 2727–2738, Jun. 2013.  
 [11] D. Sun, B. Ge, F. Z. Peng, H. Abu-Rub, D. Bi, and Y. Liu, "A new grid-connected PV system based on cascaded H-bridge quasi-Z source inverter," in *Proc. IEEE Int. Symp. Ind. Electron.*, May 28–31, 2012, pp. 951–956.  
 [12] H. Abu-Rub, A. Igbal, Sk. Moin Ahmed, F. Z. Peng, Y. Li, and B. Ge, "Quasi-Z-source inverter-based photovoltaic generation system with maximum power tracking control using ANFIS," *IEEE Trans. Sustain. Energy*, vol. 4, no. 1, pp. 11–20, Jan. 2013.  
 [13] B. Ge, H. Abu-Rub, F. Peng, Q. Lei, A. de Almeida, F. Ferreira, D. Sun, and Y. Liu, "An energy stored quasi-Z-source inverter for application to photovoltaic power system," *IEEE Trans. Ind. Electron.*, vol. 60, no. 10, pp. 4468–4481, Oct. 2013.  
 [14] H. Abu-Rub, M. Malinowski, and K. Al-Haddad, *Power Electronics for Renewable Energy Systems, Transportation and Industrial Applications*. Hoboken, NJ, USA: Wiley, 2014.  
 [15] Y. A. Mahmoud, W. Xiao, and H. H. Zeineldin, "A parameterization approach for enhancing PV model accuracy," *IEEE Trans. Ind. Electron.*, vol. 60, no. 2, pp. 5708–5716, Dec. 2013.  
 [16] D. N. Zmood and D. G. Holmes, "Stationary frame current regulation of PWM inverters with zero steady-state error," *IEEE Trans. Power Electron.*, vol. 18, no. 3, pp. 814–822, May 2003.  
 [17] Y. Liu, B. Ge, F. Z. Peng, H. Abu-Rub, A. T. de Almeida, and F. J. T. E. Ferreira, "Quasi-Z-Source inverter based PMSG wind power generation system," in *Proc. IEEE Energy Conv. Congr. Expo.*, Sep. 17–22, 2011, pp. 291–297.  
 [18] J. I. Leon, S. Vazquez, J. A. Sanchez, R. Portillo, L. G. Franquelo, J. M. Carrasco, and E. Dominguez, "Conventional space-vector modulation techniques versus the single-phase modulator for multilevel converters," *IEEE Trans. Ind. Electron.*, vol. 57, no. 7, pp. 2473–2482, Jul. 2010.  
 [19] M. A. G. de Brito, L. Galotto, L. P. Sampaio, G. de Azevedo e Melo, and C. A. Canesin, "Evaluation of the main MPPT techniques for photovoltaic applications,"

*IEEE Trans. Ind. Electron.*, vol. 60, no. 3, pp. 1156–1167, Mar. 2013.



**PULLOJU DIVYA JYOTHI** currently pursuing her M.Tech in Electrical Power Systems from JB Institute of Engineering and

Technology(UGC Autonomous), affiliated to JNTUH. She received her Bachelor degree from Christu Jyothi Institute of Technology and Science affiliated to JNTU Hyderabad in 2012 and her field Interest includes Power Systems and Power Electronics.

**E-mail:**

[divvajyothi46@gmail.com](mailto:divvajyothi46@gmail.com).



**R. Suresh Babu** pursuing Ph.D from Acharya Nagarjuna University, Guntur,

Andrapradesh. He received His M.Tech in HVE from JNTUK, in 2006, Andra pradesh. He received his Bachelor degree from ANU in 1999. He is currently working as an Associate .Prof. in EEE dept., at JB institute of Engineering and Technology from JNTU Hyderabad, India, His area of interest includes Power Systems.

**E-mail:** [sbrega123@gmail.com](mailto:sbrega123@gmail.com)



**DR. S. SIVA PRASAD** received Ph.D (Electrical) from JNTUH, Hyderabad. He received M.Tech degree from JNTU, Hyderabad

and B.Tech from SV University. He currently working as a Professor and HOD in JB Institute of Engineering and Technology (UGC Autonomous), Hyderabad, India. He received “Bharat Vibhushan Samman Puraskar” from “The Economic and Human Resource Development Association” in 2013 and received Young Investigator Award in 2012. His research areas include Power Electronics, Power Electronics & Drives, Facts Controllers.

**E-mail:** [sshivprasadeee@gmail.com](mailto:sshivprasadeee@gmail.com)